Macular Structure Parameters as an Automated Indicator of Paracentral Scotoma in Early Glaucoma

YUGO KIMURA, MASANORI HANGAI, AKIKO MATSUMOTO, TADAMICHI AKAGI, HANAKO O. IKEDA, SHINJI OHKUBO, KAZUHISA SUGIYAMA, AIKO IWASE, MAKOTO ARAIE, AND NAGAHISA YOSHIMURA

• PURPOSE: To evaluate the predictive ability of macular parameters defined in the significance map created using spectral-domain optical coherence tomography (SD-OCT) for paracentral visual field defects in early glaucoma.

• DESIGN: Prospective comparative study.

• METHODS: We studied 78 early-glaucomatous eyes of 78 patients, who underwent SD-OCT and standard automated perimetry 10-2. Macular layer parameters included the retinal nerve fiber layer (RNFL), ganglion cell layer (GCL) + inner plexiform layer (IPL), and RNFL + GCL + IPL. The minimal distance between the area with abnormal ($P < 1\%$) thickness and foveal center was defined as the shortest distance. A wider area of an abnormally thinned ($< 1\%$) region, within either an inferior or a superior hemicircle with a diameter of 6 mm centered at the fovea, was defined as the macular abnormal area. A circumpapillary RNFL parameter was defined in its 36 sectors. Areas under the receiver operating characteristic curves (ROCs) were calculated to discriminate between eyes with (n = 39) and without (n = 39) paracentral visual field defects in the central 5 degrees.

• RESULTS: Measurement reproducibility was almost perfect in the macular parameters at $P < 1\%$ (intraclass correlation, 0.907–0.942). Areas under the ROC were significantly higher ($P \leq 0.01$) in the macular parameters (0.870–0.930), including the shortest distance of GCL + IPL/RNFL + GCL + IPL, and the macular abnormal area of RNFL/GCL + IPL/RNFL + GCL + IPL than in the circumpapillary RNFL parameter (0.676). When specificity was fixed at ≥90%, the shortest distance of GCL + IPL (area under the ROC = 0.874) and the macular abnormal area of RNFL (area under the ROC = 0.894) showed sensitivities greater than 50%.

• CONCLUSIONS: Macular structural parameters defined on an SD-OCT significance map may be potentially useful predictors of the presence of paracentral scotoma. (Am J Ophthalmol 2013;156:907–917. © 2013 by Elsevier Inc. All rights reserved.)

Accepted for publication Jun 19, 2013.

From the Department of Ophthalmology and Visual Sciences, Kyoto University Graduate School of Medicine, Kyoto, Japan (Y.K., M.H., T.A., H.O.I., N.Y.); the Department of Ophthalmology and Visual Science, Kanazawa University Graduate School of Medical Science, Kanazawa, Japan (S.O., K.S.); Topcon Corporation, Tokyo, Japan (A.M.); the Tajimi Iwase Eye Clinic, Tajimi Gifu, Japan (A.I.); and the Kanto Central Hospital of the Mutual Aid Association of Public School Teachers, Tokyo, Japan (M.A.).

Inquiries to Masanori Hangai, Department of Ophthalmology and Visual Sciences, Kyoto University Graduate School of Medicine, 54 Kawahara-cho, Shogoin, Sakyo-ku, Kyoto 606-8507, Japan; e-mail: hangai@kuhp.kyoto-u.ac.jp

THE DEVELOPMENT OF PARACENTRAL SCOTOMA IN glaucoma severely threatens patients' quality of vision.[1,2] Glaucoma can affect the central or paracentral visual field (VF), even in the early stages of the disease.[3–8] It is suggested that patients with VF defects that threaten fixation should be treated more aggressively because they have an increased risk for further loss of the VF close to fixation which, in turn, is associated with the loss of visual acuity.[9] Thus, it is critical to detect VF sensitivity loss in the paracentral VF as early as possible. Early detection of paracentral VF defects helps physicians to treat their patients more effectively, such as targeting lower intraocular pressure and scheduling follow-up by standard automated perimetry (SAP) 30-2 and 24-2 programs and the SAP10-2 program.

SAP24-2 is not designed to detect paracentral scotoma effectively because it includes only 5 testing points for the central region within 5 degrees of the fixation. Although SAP10-2 allows effective detection of paracentral VF defects because it includes 25 testing points within 5 degrees, it would be difficult to perform SAP10-2 routinely for all patients with glaucoma. Thus, time-saving examinations that can predict the risk for paracentral VF defects are desirable.

Glaucomatous optic neuropathy results from retinal ganglion cell loss following damage to retinal ganglion cell axons within the optic nerve head. A 3-dB reduction of VF sensitivity within the central 10 degrees is associated with a retinal ganglion cell loss of more than 60% on SAP30-2 and 24-2.[10] Half of the retinal ganglion cells exist in the central 4.5-mm–diameter region of the macula and are arranged at a thickness of 7 to 8 cell layers at the peak; this corresponds to the thickest ganglion cell layer (GCL), which is approximately 57 to 64 μm thick at a distance of around 1 mm from the foveal center.[11–13] The GCL and retinal nerve fiber layer (RNFL) thinning in the macula is evident even in eyes with preperimetric glaucoma.[12,14,15] Although the location of retinal ganglion cells is a little displaced peripherally from the corresponding photoreceptors in the central 7.2 degrees,[16] the retinal ganglion cell loss matches well in location with the VF sensitivity loss.[17] Thus, macular thinning due

0002-9394/$36.00
http://dx.doi.org/10.1016/j.ajo.2013.06.029

to glaucomatous optic neuropathy may be a sensitive target for predicting paracentral scotoma in early glaucoma.

Spectral-domain optical coherence tomography (SD-OCT) enables 3-dimensional (3D) and high-axial resolution imaging of the macular inner retinal layers, such as the RNFL and GCL, and allows an accurate and reproducible automated thickness measurement of a single RNFL[18] or combined inner retinal layers, including the GCL.[13,14,19,20] The SD-OCT instruments statistically classify the thickness of these layers at each A-scan as abnormal, borderline or normal as compared to the confidence intervals of the built-in normative database and display a color-coded significance map in which the regions with abnormal or borderline thickness are shown in red or yellow. The significance map is useful for early diagnosis of glaucoma.[21,22] The purpose of this study was to test the predictive ability of the macular structural parameters created in an automated manner based on the significance map of the inner retinal layers on SD-OCT to detect paracentral VF defects in early glaucoma.

METHODS

THIS PROSPECTIVE, CROSS-SECTIONAL, COMPARATIVE study was carried out with approval by the institutional review board and ethics committee of Kyoto University Graduate School of Medicine and Kanazawa University Graduate School of Medical Science and adheres to the tenets of the Declaration of Helsinki. Informed consent to participate in this study was obtained from the patients or subjects after they received an explanation of the nature and possible consequences of the study.

Patients with glaucoma examined in the glaucoma clinic at the Kyoto University Hospital (Kyoto, Japan) and Kanazawa University Hospital (Kanazawa, Japan) between May 2010 and August 2012 were enrolled. All participants underwent comprehensive ophthalmic examinations, including a best-corrected visual acuity measurement using a 5-m Landolt chart; refraction; slit-lamp biomicroscopy; intraocular pressure measurements using a Goldman applanation tonometer; gonioscopy; axial length measurements by partial laser interferometry (IOLMaster, Carl Zeiss Meditec, Dublin, California, USA); dilated biomicroscopic examination; stereo disk photography with a 3D × simultaneous stereo disk camera (Nidek, Gamagori, Japan); red-free fundus imaging using a Heidelberg Retina Angiogram II (HRA2, Heidelberg Engineering, Heidelberg, Germany); and SD-OCT examination with 3D OCT-2000 (Topcon, Tokyo, Japan). SAP was performed using the 24-2 and 10-2 Swedish Interactive Threshold Algorithm (Humphrey Field Analyzer, Carl Zeiss Meditec) within 3 months of SD-OCT examination.

Inclusion criteria were glaucomatous optic neuropathy, normal open angles confirmed by gonioscopy, mean deviation (MD) on SAP24-2 < -6 dB, best corrected visual acuity of 20/25 or better in Snellen equivalent, and a spherical equivalent refractive error ≤ -6.00 diopter. Eyes with any type of vitreoretinal diseases, media opacity, or history of ocular surgery were excluded. Patients with histories of corticosteroid use and evidence of neurologic diseases or systemic disorders such as diabetes that might affect the retinal structure and VF were excluded. When both eyes were eligible, 1 eye was randomly selected for inclusion in the study.

A patient was diagnosed as having glaucomatous optic neuropathy when the optic disk had a glaucomatous appearance (diffuse or localized neuroretinal rim thinning) on stereo disk photographs or RNFL defects corresponding with the glaucomatous VF defects on red-free fundus imaging or both. Both SAP24-2 and SAP10-2 were considered reliable when fixation losses and the false-positive and false-negative rates were less than 15%. A glaucomatous VF defect was defined on SAP24-2 as (1) a glaucoma hemifield test value that was outside the normal limits; (2) at least 3 vertical, horizontal or diagonal contiguous test points within the same hemifield on the pattern deviation probability plot at $P < 5\%$, with at least 1 point at $P < 1\%$, excluding points directly above or below the blind spot; or (3) a pattern standard deviation <5% of the normal reference values, confirmed by at least 2 VF tests.

• **SD-OCT EXAMINATION:** A well-trained examiner performed SD-OCT examinations in each eye after pupil dilation with tropicamide (0.5%) and phenylephrine (2.5%). The OCT equipment has a 6-μm depth resolution in tissue, a 20-μm transverse resolution, and an A-scan acquisition rate of 50,000/second. For the macular measurement, a 3D raster scan protocol of 128 vertical B-scans was used, comprising 512 A-scans per B-scan over 65,536 samplings within a cube of 7 mm × 7 mm × 2.3 mm centered at the foveal center. For the circumpapillary RNFL measurement, a 3D raster scan protocol of 128 horizontal B-scans was used, comprising 512 A-scans per B-scan over 65,536 samplings within a cube of 6 mm × 6 mm × 2.3 mm centered at the optic disk center. Both scans took 1.3 seconds. The examiner discarded poor-quality images that had visible eye motion, blinking artifacts (discontinuous jump) or poor centration. To calculate the test-retest measurement variability, 3 scans per eye with acceptable images were obtained during the same visit.

• **MEASUREMENT ON SD-OCT:** To obtain a more accurate macular scan area, the magnification effect on lateral length was corrected in each scan by using the manufacturer's formula (a modified Littman method) based on the eye's refractive error, corneal radius and axial length. Only high-quality images, as indicated by a signal strength score (Q-factor) >65, were used for measurement.

For macular measurement, the 3D OCT built-in software was used; it automatically detects the foveal center and

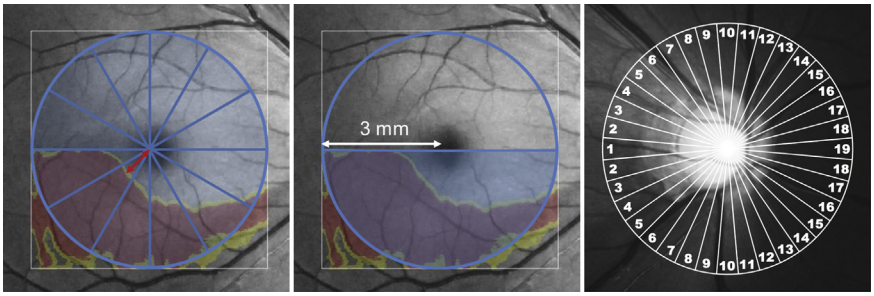

FIGURE 1. Schema for structural parameters based on the significance map of spectral-domain optical coherence tomography to indicate the proximity to the fovea of structural damages. (Left) A circle (diameter, 6 mm) and 6 spokes (radial lines) are drawn on the significance map of macular layer thickness centered at the foveal center, which creates 12 sectors of 30 degrees. The distance between the foveal center and the meeting point of each of the 360 spokes with the central edge of the abnormally (red)/borderline (yellow) thinned area is the nearest distance of macular thinning to the fovea. The nearest distances of the 360 spokes were averaged every 30 degrees to obtain the average nearest distance in each of the 12 sectors. A minimal average nearest distance among the 12 sectors was defined as the shortest distance of the abnormal macular thinning to the fovea in each eye (red double-headed arrow). (Center) The translucent semicircle area on the same significance map indicates the wider area of the abnormally thinned (< 1%, red)/borderline-thinned (< 5%, yellow) region within either an inferior or a superior hemicircle at a diameter of 6 mm. White lines indicate 6 mm × 6 mm squares that are cut out and centered on the foveal center from each scan area by 7 mm × 7 mm. (Right) The 36 sectors in a circle (diameter, 3.4 mm) were used to calculate the mean circumpapillary retinal nerve fiber layer (RNFL) thickness. The temporal position was designated as number 1 and the nasal position as number 19. The assigned numbers increase as a function of the angle from the temporal position toward the nasal position, in a clockwise or counterclockwise direction. The smallest number of sectors with abnormal thickness was used as a parameter to indicate the circumpapillary RNFL structural damages nearest to the fovea.

places a 6 mm × 6 mm square centered on the fovea. This software automatically measures the thickness of a single layer or combined layers, such as the RNFL, GCL + IPL, and RNFL + GCL + IPL (GCC). RNFL was measured as the distance between the vitreoretinal interface and the outer boundary of the RNFL, GCL + IPL between the outer boundary of the RNFL and the outer boundary of the IPL, and the GCC between the vitreoretinal interface and the outer boundary of the IPL. The software compares measurements to the corresponding confidence interval of the device's normative database[23,24] and displays three color-coded significance maps. Regions within the normal range ($P > 5\%$ and $P < 95\%$), those with borderline thinning ($1\% < P < 5\%$), and those with abnormal thinning ($P < 1\%$) are shown in green, yellow, and red, respectively (Figure 1 and Figure 2).

For circumpapillary RNFL thickness measurements, the 3D OCT built-in software automatically detects the center of the optic disk and places around it a 3.4-mm–diameter calculation circle consisting of 1,024 A-scans. The circumpapillary RNFL thickness was measured as the distance between the anterior and posterior boundaries of the RNFL delineated by the computer algorithm. To assess regional circumpapillary RNFL thickness abnormalities, the 3D OCT built-in software provides a color-coded significance map with 4, 12 or 36 equal-part sectors. Abnormal circumpapillary RNFL thickness in each circumpapillary RNFL sector is displayed as red (<1%), yellow (≥1% and <5%), green ($P > 5\%$ and ≤95%), or white (>95%) compared to the confidence intervals of the normative database (Figure 2).

• **PARAMETERS INDICATIVE OF THE CENTRALITY OF STRUCTURAL DAMAGES TO THE FOVEA:** We built a prototype software based on the 3D OCT built-in software to create two macular structural parameters that indicated the extent of macular thinning to the fovea on the significance map for the RNFL, GCL + IPL, and RNFL + GCL + IPL. One was the nearest distance of the abnormally thinned (<1%) or borderline-thinned (<5%) region to the foveal center on significance map (Figure 2). To evaluate this, the software automatically drew 360 spokes that extended from the foveal center at every 1 degree in a counterclockwise direction and measured the distance between the foveal center and the meeting point of each spoke with the central edge of the abnormally or borderline-thinned area as the nearest distance of macular thinning to the fovea. The nearest distances of the 360 spokes were averaged every 30 degrees to obtain the average nearest distance in each of the 12 sectors. A minimal nearest distance among the 12 sectors was defined as the shortest distance of the macular thinning to the fovea in each eye. A second parameter was the wider area of abnormally thinned (<1%) or borderline-thinned (<5%) regions within an inferior or a superior hemicircle with a diameter of 6 mm, defined as the macular abnormal area (Figure 1). Our prototype software automatically calculated the parameters of the shortest distance and the macular abnormal area.

We used 36 sectors to create a circumpapillary RNFL parameter that indicated the centrality of the retinal ganglion cell damages to the fovea (Figures 1 and 2). We designated the temporal position as number 1 and the nasal position as number 19. Thus, the assigned numbers

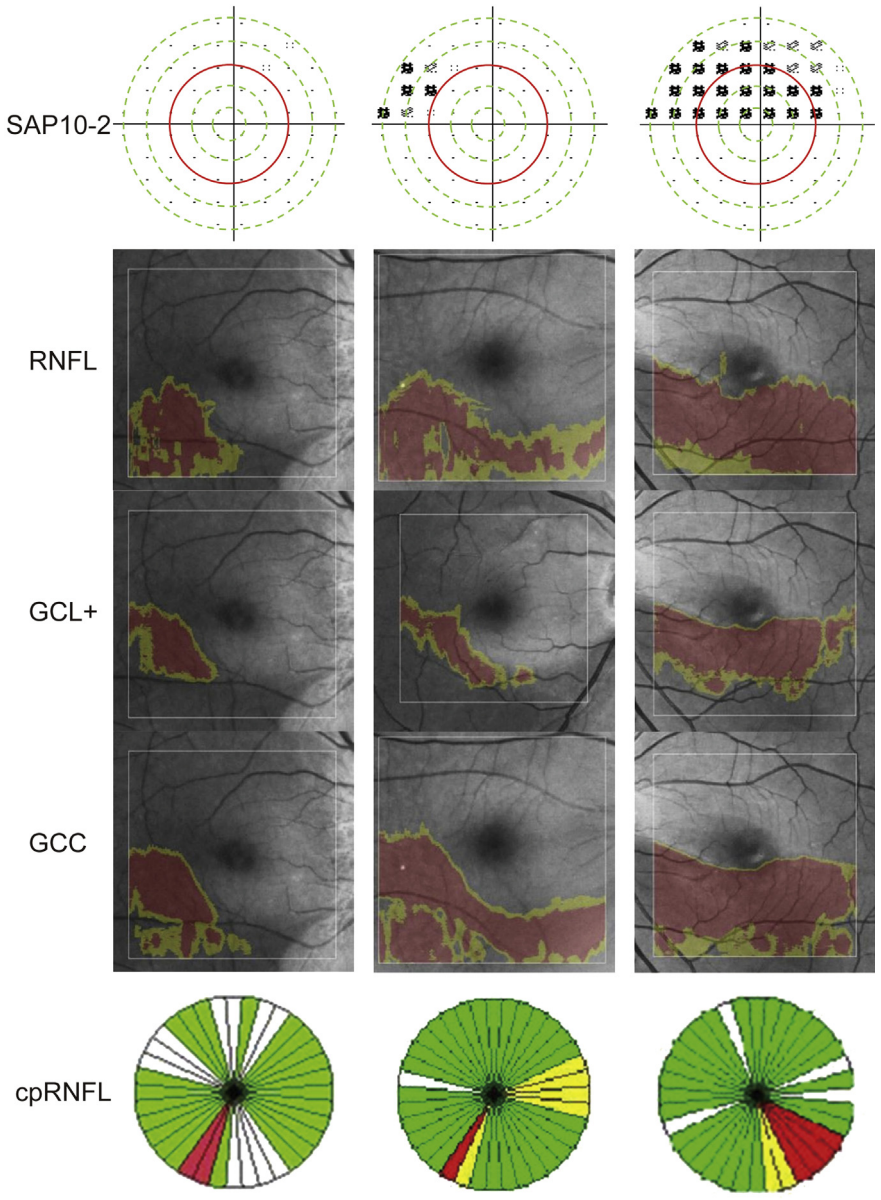

FIGURE 2. Early glaucomatous cases with 3 types of visual field defects on 10-2 testing (Top) Pattern deviation maps in standard automated perimetry 10-2 and 5 concentric circles (green or red lines) with test points grouped according to the distance from the fixation point. The 5 groups were numbered from 1 to 5 as a function of the distance from the fixation point. (Second, third and fourth rows) Significance maps of the macular retinal nerve fiber layer (RNFL, second row), ganglion cell layer + inner plexiform layer (third row), and RNFL + ganglion cell layer + inner plexiform layer (ganglion cell complex, fourth row). White lines indicate 6-mm × 6-mm squares cut out and centered on the foveal center from each scan area by 7 mm × 7 mm. (Bottom) Color-coded significance maps for 36-sector analysis of the circumpapillary RNFL thickness. Abnormal thickness in each sector is displayed as red (< 1%), yellow (≥1% and < 5%), green (P > 5% and ≤95%), and white (> 95%) compared to the confidence intervals of the same normative database. (Left) A case without glaucomatous visual field (VF) defects on 10-2 testing (control group). (Center) A case with glaucomatous VF defects outside the number 3 concentric circle. (Right) A case with glaucomatous VF defects on and inside the number 3 concentric circle (the paracentral VF defect group). The macular VF defect group includes eyes with (right) and without (center) a paracentral VF defect.

increased as a function of the angle from the temporal position toward the nasal position, in a clockwise or counterclockwise direction (Figure 1). The smallest number of sectors with abnormal thickness in each eye should have indicated structural damages nearest to the fovea (Figure 2). We used the lowest number of sectors with abnormal thickness as a structural parameter to detect paracentral scotoma in circumpapillary RNFL analysis.

• **REPRODUCIBILITY:** The reproducibility of macular measurements with 3D OCT was assessed in 28 eyes of 28 patients with glaucoma. To assess intervisit reproducibility, 3D OCT examinations were performed at 3 visits within 3 months after the initial visit. The intraclass correlation coefficient (ICC) and the Kendall coefficient of concordance were calculated to assess the intervisit reproducibility of continuous and categoric parameters, respectively. The coefficients of variation were calculated to assess intervisit variability.

• **CLASSIFICATION OF VISUAL FIELD DEFECTS ACCORDING TO PROXIMITY TO THE FIXATION POINT IN 10-2 TESTING:** Glaucomatous VF defects on SAP10-2 were defined as follows: the presence of more than 1 cluster of at least 3 vertical, horizontal or diagonal contiguous test points at $P < 5\%$ within the same hemifield on the pattern deviation probability plot, with at least 1 point at $P < 1\%$, and the VF defects were located in the same hemifield as the VF defects in the SAP24-2. The SAP10-2 results were confirmed by at least 2 VF tests performed within 6 months, and the results of the 10-2 test performed closer to the visit for the SD-OCT examination were used for analysis.

The distance of the test points from the fixation points on SAP10-2 on the pattern deviation probability plot were grouped by five concentric circles centered at fixation, each of which passed the four test points nearest to the horizontal axis (Figure 2). The test points located between neighboring two circles or on the outer circle were regarded as a group with a similar distance to a fixation point. The five groups were numbered from 1 to 5 as a function of the distance from the fixation point. The number of the nearest concentric circle, including abnormal test points at $P < 1\%$, was regarded as the nearest concentric circle in each eye. When glaucomatous VF defects were absent on SAP10-2, the number of the nearest concentric circle was considered to be 5 so as to calculate its correlations with SD-OCT parameters.

The study eyes were classified into three groups when they had the same VF defect pattern on two consecutive SAP10-2 tests. VF defects on SAP10-2 were classified into three patterns according to the proximity of the significant VF defects to the fixation point on the pattern-deviation probability plot. The paracentral VF defect pattern (right panel, Figure 2) was defined as glaucomatous VF defects with more than one point at $P < 1\%$ on or inside the number 3 concentric circle (red circle, Figure 2, approximately 5 degrees from the fixation point). The macular VF defect pattern was defined as glaucomatous VF defects on SAP10-2. The group with this pattern included eyes with (right panel, Figure 2) and without (center panel, Figure 2) a paracentral VF defect. The third pattern was defined as no glaucomatous VF defects on SAP10-2 (left panel, Figure 2).

• **STATISTICAL ANALYSIS:** Differences in parameters between the two groups were compared by using unpaired *t* tests or the Mann-Whitney U test, and differences among the 3 groups were compared by analysis of variance (ANOVA) followed by the Tukey post hoc test. Spearman rank correlation coefficients were calculated for the analysis of correlation between the structural and VF parameters. The diagnostic accuracy was determined by computing the area under the ROC, and the sensitivity at fixed specificities was computed to discriminate between eyes with and without macular or paracentral VF defects. We calculated criteria to determine the optimal cutoff point for the parameters that could be used to distinguish between the presence and absence of macular or paracentral VF defects. The method of Delong and associates[25] was used to compare the areas under the ROC between parameters. The unpaired *t* test scores, Mann-Whitney U test, ANOVA, Spearman rank correlation coefficients, ICC, and Kendall coefficient of concordance were calculated using the SPSS17 statistics software program (SPSS, Chicago, Illinois, USA), and the areas under the ROC were compared using MedCalc12 (MedCalc, Mariakerke, Belgium). *P* values <0.05 were considered statistically significant.

RESULTS

IN 99 JAPANESE PATIENTS, 114 EYES MET THE INCLUSION criteria. Of these, 11 eyes were excluded because they had undergone cataract surgery (8 eyes) or had had vitreoretinal diseases, such as epiretinal membrane (1 eye), diabetic retinopathy (1 eye), or superior segmental optic hypoplasia (1 eye). The random selection of 1 eye in patients with 2 eligible eyes resulted in the exclusion of 20 eyes. Furthermore, 5 eyes were excluded because the Q factor of the SD-OCT image was <60. Thus, 78 eyes of 78 patients were used for the current study. The demographics of all the study eyes and of each group are shown in Table 1. Signal-strength values of the SD-OCT scans are also shown in Table 1. No significant differences were found among the three groups except for the SAP24-2 and 10-2 indices. The group without any macular VF defect had better SAP indices than the other two groups, but there were no significant differences between the two groups with macular VF defect and paracentral VF defect.

Glaucomatous VF defects on SAP10-2 were found in both hemifields in 7 (9%) eyes and were limited to the superior and inferior hemifields in 38 (48.7%) and 7 (9.0%) eyes, respectively. Of 78 eyes, 39 (50%) had paracentral VF defects and 52 (66.7%) had macular VF defects on SAP10-2. Of 39 eyes with paracentral VF defects on SAP10-2, glaucomatous VF defects involved the innermost test points of SAP24-2 at $P < 1\%$ in 31 (79.5%) eyes and did not involve the same in 9 (23.1%) eyes.

Measurement reproducibility was almost perfect in macular parameters, including the shortest distance, at $P < 1\%$ (ICC, 0.907–0.921); the macular abnormal area, at $P < 1\%$ (ICC, 0.920–0.942); and the circumpapillary

TABLE 1. Demographics of Study Patients with Early Glaucoma and Signal Strength of Spectral-Domain Optical Coherence Tomography Scans

		Classification of VF defect defined on SAP10-2			
	All Eyes (n = 78)	Eyes with Macular VF Defect (n = 52)	Eyes with Paracentral VF Defect (n = 39)	Eyes without Macular VF Defect (n = 26)	*P* Value
Age	56.1 (11.8)	55.0 (12.4)	54.5 (12.4)	57.9 (10.8)	0.54[a]
Gender (men/women)	36/42	20/32	15/24	10/16	1.0[b]
Refractive error (D)	−2.2 (2.2)	−2.2 (2.1)	−2.5 (2.1)	−2.2 (2.4)	0.86[a]
Axial length (mm)	24.6 (1.2)	24.5 (1.2)	24.4 (1.0)	24.8 (1.2)	0.33[a]
IOP (mm Hg)	15.6 (2.4)	15.7 (2.2)	15.9 (2.1)	15.6 (2.8)	0.81[a]
SAP 24-2					
MD (dB)	−2.0 (2.3)	−2.4 (2.4)[c]	−2.7 (2.6)[d]	−1.1 (1.9)[c,d]	0.02[a]
PSD (dB)	3.9 (2.6)	4.4 (4.8)[e]	4.7 (2.8)[f]	2.2 (1.6)[e,f]	0.003[a]
SAP 10-2					
MD (dB)	−2.6 (3.4)	−3.8 (3.7)[g]	−4.8 (3.7)[h]	−0.5 (0.8)[g,h]	<0.001[a]
PSD (dB)	4.3 (4.2)	3.2 (6.0)[i]	6.8 (4.5)[j]	1.2 (0.2)[i,j]	0.002[a]
Signal strength of SD-OCT scans					
Macular scan	74.3 (6.4)	75.3 (6.8)	75.8 (6.2)	73.0 (5.6)	0.23[a]
Circumpapillary RNFL scan	74.4 (6.6)	74.8 (6.7)	74.3 (6.1)	73.6 (6.7)	0.79[a]

D = diopter; IOP = intraocular pressure; MD = mean deviation; PSD = pattern standard deviation; RNFL = retinal nerve fiber layer; SAP = standard automated perimetry; SD-OCT = spectral-domain optical coherence tomography; VF = visual field.

Decimal data are mean (standard deviation).

[a]Analysis of variance followed by Tukey post hoc test.

[b]χ^2 test.

[c]$P = 0.03$.

[d]$P = 0.02$.

[e]$P < 0.001$.

[f]$P < 0.001$.

[g]$P < 0.001$.

[h]$P < 0.001$.

[i]$P = 0.007$ for eyes with a macular VF defect vs those without any macular VF defect.

[j]$P < 0.001$ for eyes with a paracentral VF defect vs those without any macular VF defect.

Notes: Macular VF defect is defined as glaucomatous VF defects on SAP10-2; paracentral VF defect is defined as glaucomatous VF defects with more than 1 point at $P < 1\%$ within the 24 innermost test points on SAP10-2.

RNFL at $P < 1\%$ and $P < 5\%$ (Kendall coefficient of concordance, 0.913 and 0.947, respectively) (Table 2). However, the shortest distance (ICC: RNFL, 0.758, and GCL + IPL, 0.656) and abnormal area (RNFL, 0.880, and GCL + IPL, 0.896) at $P < 5\%$ exhibited relatively low measurement reproducibility (Table 2); therefore, subsequent analyses and comparisons of macular and circumpapillary RNFL parameters were made at $P < 1\%$.

A macular abnormal area at $P < 1\%$ was detected within the 6-mm circle in all study eyes, and sectorial circumpapillary RNFL thickness at $P < 1\%$ was detected in 62 (79.5%) eyes. The hemiretinal location of the macular abnormal area at $P < 1\%$ was matched to that of the shortest distance at $P < 1\%$ in all eyes. The macular abnormal area at $P < 1\%$ and the shortest distance at $P < 1\%$ were superiorly located in 55 of 78 eyes (70.5%) and inferiorly in 23 eyes (29.5%).

All the mean values of the macular parameters differed significantly between eyes with and without paracentral VF defects ($P \leq 0.009$) (Table 3). The differences between eyes with and without macular VF defects were statistically significant ($P \leq 0.01$) for all macular parameters except the shortest distance in RNFL and GCL + IPL thickness of the thinner hemisphere (Table 3). The mean number of nearest abnormal sectors of circumpapillary RNFL was significantly different between eyes with and without paracentral VF defects and between eyes with and without macular VF defects ($P = 0.04$ and 0.02, respectively; Table 3).

All of the macular parameters were significantly correlated with all types of the SAP10-2 parameters except for the shortest distance versus MD for RNFL (Table 4). Overall, the shortest distances and macular abnormal area parameters tended to exhibit better correlations (higher correlation coefficients) with the nearest concentric circles indicating the distance of abnormal test points at $P < 1\%$ from the fixation point than those with global parameters, such as number of points at $P < 1\%$ and MD values.

The area under the ROC and the sensitivities (%) at fixed specificities (80% and 90%) to detect macular and

TABLE 2. Measurement Reproducibility and Variability for Macular Structural Parameters as Measured with Three-dimensional Spectral-domain Optical Coherence Tomography in Eyes with Early Glaucoma

Parameters	Coefficient of Reproducibility	CV (%)
Shortest distance at $P < 1\%$ (mm)		
RNFL	0.921[a]	4.3
GCL + IPL	0.915[a]	5.8
RNFL + GCL + IPL	0.907[a]	4.4
Shortest distance at $P < 5\%$ (mm)		
RNFL	0.758[a]	5.4
GCL + IPL	0.656[a]	7.1
RNFL + GCL + IPL	0.989[a]	3.6
Macular abnormal area at $P < 1\%$ (mm^2)		
RNFL	0.920[a]	5.8
GCL + IPL	0.921[a]	3.3
RNFL + GCL + IPL	0.942[a]	2.7
Macular abnormal area at $P < 5\%$ (mm^2)		
RNFL	0.880[a]	5.4
GCL + IPL	0.896[a]	5.0
RNFL + GCL + IPL	0.967[a]	1.1
Circumpapillary RNFL at $P < 1\%$	0.913[b]	2.3
Circumpapillary RNFL at $P < 5\%$	0.947[b]	1.0

CV = coefficient of variation; GCL = ganglion cell layer; IPL = inner plexus layer; RNFL = retinal nerve fiber layer.
[a]ICC = intraclass correlation.
[b]Kendall coefficient of concordance.

paracentral VF defects are shown in Table 5. Overall, the areas under the ROC of individual macular parameters were better in the paracentral VF defects (ranging from 0.763 to 0.894) than in the macular VF defects (ranging from 0.589 to 0.788).

In the 62 eyes that had abnormal ($P < 1\%$) sectors in the 36 circumpapillary RNFL sectors, the areas under the ROC of the shortest distance to detect macular or paracentral VF defects were 0.550/0.778 in the RNFL, 0.750/0.901 in the GCL + IPL, and 0.713/0.888 in the RNFL + GCL + IPL. The areas under the ROC of the abnormal area to detect macular or paracentral VF defects were 0.812/0.930 in the RNFL, 0.796/0.870 in the GCL + IPL, and 0.826/0.898 in the RNFL + GCL + IPL. The areas under the ROC to detect paracentral VF defects were higher in the shortest distance of GCL + IPL ($P = 0.002$) and RNFL + GCL + IPL ($P = 0.005$), and macular abnormal area of RNFL ($P < 0.001$), GCL + IPL ($P = 0.01$), and RNFL + GCL + IPL ($P = 0.006$) than in the number of the nearest abnormal sectors of circumpapillary RNFL.

The areas under the ROC to detect macular or paracentral VF defects were compared between retinal layers for each macular parameter (Table 5); GCL + IPL (0.008/0.008) and RNFL + GCL + IPL (0.003/0.020) showed significantly higher areas under the ROC ($P = 0.008$/0.008 and 0.03/0.02, respectively) than RNFL for the shortest distance, but no significant differences were found between layers for the macular abnormal area. The GCL + IPL showed higher area under the ROC to detect macular or paracentral VF defects than RNFL + GCL + IPL for the shortest distance, but these differences were not statistically significant ($P = 0.05$). No significant differences were found between retinal layers for the area under the ROC of the macular abnormal area to detect macular or paracentral VF defects.

The areas under the ROC to detect macular or paracentral VF defects were compared in terms of the macular parameters for each retinal layer (Table 5); the macular abnormal area showed significantly greater area under the ROC of the RNFL to detect macular or paracentral VF defects ($P < 0.001$/0.001) than the shortest distance, and the macular abnormal area showed significantly greater area under the ROC of the RNFL + GCL + IPL to detect macular VF defects ($P = 0.04$) than the shortest distance. However, no significant differences were found for the area under the ROC of GCL + IPL or RNFL + GCL + IPL to detect macular or paracentral VF between the shortest distance and macular abnormal area.

When the specificity was fixed at ≥90%, only the shortest distance of GCL + IPL and the macular abnormal area for RNFL showed a sensitivity >50% for detecting paracentral VF defects (Table 5).

DISCUSSION

ALTHOUGH NUMEROUS STUDIES HAVE INVESTIGATED THE ability of structural parameters to detect early glaucoma, few data are available regarding the ability of structural parameters to indicate the presence of paracentral scotoma. Although SAP10-2 is useful for classifying the risk that VF defects threaten fixation, routinely performing SAP10-2 in clinics is difficult. Earlier studies have shown that local thickness of GCL + IPL correlates well with local sensitivity loss in glaucoma on SAP10-2,[16,26] suggesting that automatically measured inner retinal layers, including GCL + IPL, could indicate the presence of paracentral VF defects detectable on SAP10-2. In the current study, we screened macular structural parameters defined on the SD-OCT significance map for detecting macular and paracentral VF defects classified on SAP10-2, and we found that these macular parameters more accurately detected paracentral VF defects than did the circumpapillary RNFL parameter.

Earlier studies also showed a spatial correlation between the locations of abnormal circumpapillary RNFL thickness and SAP24-2 or 30-2.[27,28] However, in the current study, the circumpapillary RNFL parameter was less accurate in detecting macular or paracentral VF defects than were the macular parameters. This difference may be attributable to the anatomic differences between the

TABLE 3. Mean Macular Parameters at $P < 1\%$ According to the Proximity of Visual Field Defects to the Fixation Point and Number of Nearest Abnormal Sector at $P < 1\%$ of Circumpapillary Retinal Nerve Fiber Layer in Eyes with Early Glaucoma

		Macular VF Defect Defined on SAP10-2			Paracentral VF Defect Defined on SAP10-2		
Layers	All Eyes (N = 78)	Presence (n = 52)	Absence (n = 26)	*P* Value[a]	Presence (n = 39)	Absence (n = 39)	*P* Value[a]
Shortest distance (mm)							
RNFL	1.06 (0.65)	0.99 (0.54)	1.20 (0.82)	0.18	0.81 (0.28)	1.35 (0.79)	<0.001
GCL + IPL	1.1 (0.85)	0.84 (0.63)	1.60 (1.02)	<0.001	0.59 (0.22)	1.60 (0.95)	<0.001
RNFL + GCL + IPL	0.96 (0.66)	0.82 (0.53)	1.22 (0.80)	0.01	0.62 (0.22)	1.29 (0.77)	<0.001
Macular abnormal area (mm^2)							
RNFL	6.0 (3.61)	7.22 (3.07)	3.56 (3.39)	<0.001	8.43 (2.30)	3.56 (2.98)	<0.001
GCL + IPL	4.53 (3.08)	5.54 (2.81)	2.50 (2.65)	<0.001	6.41 (2.40)	2.65 (2.50)	<0.001
RNFL + GCL + IPL	7.38 (3.85)	8.67 (3.31)	4.82 (3.72)	<0.001	9.77 (2.43)	5.00 (3.51)	<0.001
No. of nearest abnormal sector of circumpapillary RNFL	5.58 (1.76) (n = 62)	5.36 (1.78) (n = 47)	6.27 (1.71) (n = 15)	0.04[b]	5.17 (1.71) (n = 34)	6.07 (1.72) (n = 28)	0.02[b]

GCL = ganglion cell layer; IPL = inner plexiform layer; RNFL = retinal nerve fiber layer; SAP = standard automated perimetry; VF = visual field.

Macular VF defects are defined as glaucomatous VF defects on SAP 10-2. Paracentral VF defects are defined as glaucomatous VF defects with more than 1 point at $P < 1\%$ within the 24 innermost test points on SAP10-2.

[a]Unpaired *t* test.

[b]Mann-Whitney U test.

Notes: Decimal data are mean (standard deviation).

TABLE 4. Correlation Between Macular Parameters at $P < 1\%$ and Visual Field (10-2) Parameters in 78 subjects with Early Glaucoma

	SAP10-2 Parameters					
	Total Deviation Map					
	No. of Nearest Concentric Circles with Points at $P < 1\%$		Number of Points at $P < 1\%$		MD	
Layer(s)	rs	*P* value	rs	*P* value	rs	*P* value
Shortest distance (mm)						
RNFL	0.37	0.001	−0.25	0.040	0.21	0.07
GCL + IPL	0.58	<0.001	−0.46	<0.001	0.41	<0.001
RNFL + GCL + IPL	0.51	<0.001	−0.4	<0.001	0.35	0.001
Macular abnormal area (mm^2)						
RNFL	−0.60	<0.001	0.56	<0.001	−0.47	<0.001
GCL + IPL	−0.55	<0.001	0.51	<0.001	−0.45	<0.001
RNFL + GCL + IPL	−0.55	<0.001	0.55	<0.001	−0.47	<0.001
No. of nearest abnormal sectors of circumpapillary RNFL (n = 62)	0.341	0.007	−0.16	0.22	0.235	0.07

GCL = ganglion cell layer; IPL = inner plexiform layer; MD = mean deviation; No. = number; RNFL = retinal nerve fiber layer; rs = correlation coefficients; SAP = standard automated perimetry.

Note: Spearman rank correlation was used to correlate the macular parameters measured with spectral-domain optical coherence tomography (SD-OCT) and HFA 10-2 parameters.

RNFL and the GCL. The GCL is composed primarily of the bodies of the retinal ganglion cells, which connect with corresponding photoreceptors with a slight peripheral displacement.[16] The thinning of the GCL in a localized region indicates the loss of retinal ganglion cells in the same region, which leads to retinal sensitivity loss almost in the same region. In contrast, the circumpapillary RNFL includes the axons of the retinal ganglion cells distributed along the course of the RNF bundles; some axons come from near the fovea, whereas other axons come from a wider location distant from the fovea. Thus, circumpapillary RNFL thinning cannot indicate retinal ganglion cell loss in a specific region.

The area under the ROC analysis revealed several candidates for macular parameters that may be useful in detecting paracentral VF defects (area under the ROC > 0.85):

TABLE 5. Areas under the Receiver Operating Characteristic Curve, Sensitivity at Fixed Specificity, and Criterion for the Macular Parameters at $P < 1\%$ to Detect Macular/Paracentral Visual Field Defects on 10-2 Perimetry in Eyes with Early Glaucoma

	Macular Visual Field Defect			Paracentral Visual Field Defect		
		Sensitivity at Fixed Specificity			Sensitivity at Fixed Specificity	
Parameters	Area under the ROC	≥80.0%	≥90.0%	Area under the ROC	≥80.0%	≥90.0%
Shortest distance (mm)						
RNFL	0.589[a,c,d]	30.8	25.0	0.763[e,f,g]	43.6	41.0
GCL + IPL	0.738[c]	51.9	5.77	0.874[f]	76.9 (0.78 mm)	51.3 (0.51 mm)
RNFL + GCL + IPL	0.680[b,d]	46.2	5.77	0.842[g]	69.2	46.15
Macular abnormal area (mm^2)						
RNFL	0.784[a]	46.2	34.6	0.894[e]	89.7 (42.0%)	53.8 (59.3%)
GCL + IPL	0.788	78.8 (23.4%)	28.8	0.857	82.1 (31.1%)	35.9
RNFL + GCL + IPL	0.786[b]	73.1	34.6	0.870	76.9 (70.0%)	46.2
No. of nearest abnormal sectors of circumpapillary RNFL (n = 62)	0.678	23.4	14.8	0.676	23.5	11.8

GCL = ganglion cell layer; IPL = inner plexiform layer; RNFL = retinal nerve fiber layer; ROC = receiver operating characteristic curve.
[a] $P < 0.001$ for shortest distance vs macular abnormal area for RNFL.
[b] $P = 0.04$ for shortest distance vs macular abnormal area for RNFL + GCL + IPL.
[c] $P = 0.008$ for RNFL vs GCL + IPL for shortest distance.
[d] $P = 0.03$ for RNFL vs RNFL + GCL + IPL for shortest distance.
[e] $P = 0.001$ for shortest distance vs macular abnormal area for RNFL.
[f] $P = 0.008$ for RNFL vs GCL + IPL for shortest distance.
[g] $P = 0.02$ for RNFL vs RNFL + GCL + IPL for shortest distance.
Note: Criterion is shown in parenthesis only for the parameters with sensitivity ≥75% at fixed specificity ≥80.0% and with sensitivity ≥50% at fixed specificity ≥90.0%. Criterion for area parameters is shown as the percent of the area at $P < 1\%$ against the area within the hemicircle.

the shortest distance of the GCL + IPL and the macular abnormal area of the RNFL, the GCL + IPL, and the RFNL + GCL + IPL. Among these parameters, the shortest distance of the GCL + IPL and the macular abnormal area of the RNFL had sensitivities ≥50% when specificity was fixed at ≥90%. In general, the sensitivity at a high specificity is important for useful clinical parameters. We next calculated the optimal cutoff point for these selected macular parameters. For example, the optimal cutoff point suggests that the area at $P < 1\%$ in the GCL + IPL significance map rarely involves the fovea (diameter, 1 mm) in eyes without paracentral VF defects, and half of the eyes with paracentral VF defects have an abnormal area that involves the fovea (shortest distance of the GCL + IPL criterion: 0.51 mm at sensitivity 51.3% and specificity ≥90%). Similarly, nearly 60% of glaucomatous eyes with paracentral VF defects have the abnormal area in more than half of the macula (macular abnormal area of the NFL criteria: 59.3% at a sensitivity of 53.8% and a specificity of ≥90%). Thus, these optimal cutoff points might be useful in determining the risk for paracentral scotoma based on the significance map.

We did not find macular structural parameters with area under the ROC values higher than 0.9. In particular, GCL + IPL was expected to reflect macular retinal ganglion cell damage in situ more accurately than RNFL + GCL + IPL, as mentioned above, but did not outperform RNFL + GCL + IPL in the area under the ROC. A possible reason for this may be that GCL + IPL measurements were more variable than measurements of RNFL + GCL + IPL. Another possible reason may be the degree of correlation between macular structural parameters and VF parameters. The macular structural parameters significantly correlated with the nearest concentric circles in all layers but not with the other VF parameters, including the number of test points at $P < 1\%$ or MD values. Although this finding supports the potential ability of macular structural parameters to indicate the proximity of the abnormal VF test points to the fixation point, the correlation coefficients were not as high as expected, ranging from 0.4 to 0.58 for the shortest distance and from −0.61 to 0.55 for the area parameters. We speculate that this is because our definition of the parameters depended on the area with abnormal thinning compared to the built-in normative database, but it did not indicate the severity of the thinning of each layer within the abnormal area. A comparison of parameters identified using the significance map and sector-based real-thickness values, with regard to their ability to discriminate eyes with and without paracentral scotoma, is required.

In some previous studies, focal loss volume (FLV) outperformed macular thickness of RNFL + GCL + IPL with regard to discriminating between early glaucomatous and normal eyes by using RTVue (Optovue, Fremont, California, USA).[29,30] The area under the ROC might be

improved if we use a parameter such as FLV based on percentage of loss from a normative database.

Considerable macular RNFL and GCL thinning occurs in glaucomatous eyes without VF defects.[12] This observation may be attributable to the following two causes. First, it indicates that even if the area near the fovea has abnormal RNFL and GCL thinning, the damage does not necessarily cause detectable VF defects at the corresponding test points. In other words, the macular structural parameters might have the ability to detect subclinical (preperimetric) abnormalities of the RNFL and GCL near the fovea that will lead to the development of detectable VF defects near fixation in the future. Second, interindividual variability of each macular parameter in normal subjects may also be responsible for the finding.[13] Longitudinal studies are required to evaluate this possibility.

Our study included a greater number of eyes with abnormal macular areas ($P < 1\%$) and shortest distances ($P < 1\%$) in the superior hemisphere rather than in the inferior hemisphere. This does not appear to be consistent with the typical topography of glaucomatous damage shown in most previous studies, in which inferior structural damage is more common than superior damage. Our finding would probably remain applicable to glaucomatous patients with the typical topography associated with glaucomatous damage because the spatial relationship between structural and perimetric damage in the macula is probably identical between the superior and inferior hemispheres, but this remains to be confirmed.

In conclusion, our results suggest that the macular structural parameters defined on the significance map of SD-OCT can potentially predict the presence of paracentral VF defects on SAP10-2, even though the predictive power was not excellent, probably because of low correlations between the macular structural parameters and the VF parameters. Among the candidate parameters, the shortest distance of GCL + IPL and the macular abnormal area of the RNFL at $P < 1\%$ appeared to be the most promising indicators of paracentral scotoma. Because each type of SD-OCT instrument can create a significance map with its software, similar software functionality with regard to automatic calculation of the shortest distance and macular abnormal area presented in the current study could be developed for all SD-OCT instruments. In addition, our results provide the reference border for the shortest distance and the reference percent of the abnormal region, which clinicians may use to assess quickly the risk for paracentral scotoma. Further studies to enhance predictive power are warranted, prior to application of the macular structural parameters investigated herein for the management of patients with glaucoma, particularly as one of the indicators for performing SAP10-2.

ALL AUTHORS HAVE COMPLETED AND SUBMITTED THE ICMJE FORM FOR DISCLOSURE OF POTENTIAL CONFLICTS OF INTEREST, and the following were reported. Dr Hangai is a paid advisory board member for Nidek Co and received consulting fees from Topcon Corp and research funding from Nidek Co, Topcon Corp, and Canon Inc. Dr Sugiyama is a paid advisory board member for Nidek Co. Dr Iwase is a paid advisory board member for Kowa and received research funding from Topcon Corp and Carl Zeiss Meditec Inc. Dr Araie is a paid advisory board member for Topcon Corp. Dr Matsumoto is an employee of Topcon Corp. Dr Yoshimura is a paid advisory board member for Nidek Co and received research funding from Nidek, Topcon, and Canon. The other authors have no financial disclosures. This research was supported in part by the Grant-in-Aid for Scientific Research (20592038) from the Japan Society for the Promotion of Science, Tokyo, Japan. Design of study (Y.K., M.H., A.I., M.A.); Data collection (Y.K., T.A., H.O.I., S.O., K.S.); Analysis and interpretation of data (Y.K., A.M., T.A., H.O.I.); Preparation of manuscript (Y.K., M.H.); Critical revision of manuscript (KS, AI, MA, NY); and Final approval of manuscript (Y.K., M.H., A.M., T.A., H.O.I., S.O., K.S., A.I., M.A., N.Y.).

REFERENCES

1. Kolker AE. Visual prognosis in advanced glaucoma: a comparison of medical and surgical therapy for retention of vision in 101 eyes with advanced glaucoma. *Trans Am Ophthalmol Soc* 1977;75:539–555.
2. Coeckelbergh TR, Brouwer WH, Cornelissen FW, Van Wolffelaar P, Kooijman AC. The effect of visual field defects on driving performance: a driving simulator study. *Arch Ophthalmol* 2002;120(11):1509–1516.
3. Stamper RL. The effect of glaucoma on central visual function. *Trans Am Ophthalmol Soc* 1984;82:792–826.
4. Anctil JL, Anderson DR. Early foveal involvement and generalized depression of the visual field in glaucoma. *Arch Ophthalmol* 1984;102(3):363–370.
5. Koseki N, Araie M, Yamagami J, Suzuki Y. Sectorization of central 10-degree visual field in open-angle glaucoma: an approach for its brief evaluation. *Graefes Arch Clin Exp Ophthalmol* 1995;233(10):621–626.
6. Schiefer U, Papageorgiou E, Sample PA, et al. Spatial pattern of glaucomatous visual field loss obtained with regionally condensed stimulus arrangements. *Invest Ophthalmol Vis Sci* 2010;51(11):5685–5689.
7. Sihota R, Gupta V, Tuli D, Sharma A, Sony P, Srinivasan G. Classifying patterns of localized glaucomatous visual field defects on automated perimetry. *J Glaucoma* 2007;16(1):146–152.
8. Kimura Y, Hangai M, Morooka S, et al. Retinal nerve fiber layer defects in highly myopic eyes with early glaucoma. *Invest Ophthalmol Vis Sci* 2012;53(10):6472–6478.
9. Membrey WL, Poinoosawmy DP, Bunce C, Fitzke FW, Hitchings RA. Comparison of visual field progression in patients with normal pressure glaucoma between eyes with and without visual field loss that threatens fixation. *Br J Ophthalmol* 2000;84(10):1154–1158.
10. Garway-Heath DF, Caprioli J, Fitzke FW, Hitchings RA. Scaling the hill of vision: the physiological relationship between light sensitivity and ganglion cell numbers. *Invest Ophthalmol Vis Sci* 2000;41(7):1774–1782.

11. Curcio CA, Allen KA. Topography of ganglion cells in human retina. *J Comp Neurol* 1990;300(1):5–25.
12. Nakano N, Hangai M, Nakanishi H, et al. Macular ganglion cell layer imaging in preperimetric glaucoma with speckle noise-reduced spectral domain optical coherence tomography. *Ophthalmology* 2011;118(12):2414–2426.
13. Ooto S, Hangai M, Tomidokoro A, et al. Effects of age, sex, and axial length on the three-dimensional profile of normal macular layer structures. *Invest Ophthalmol Vis Sci* 2011; 52(12):8769–8779.
14. Tan O, Chopra V, Lu AT, et al. Detection of macular ganglion cell loss in glaucoma by Fourier-domain optical coherence tomography. *Ophthalmology* 2009;116(12):2305–2314.
15. Kotera Y, Hangai M, Hirose F, Mori S, Yoshimura N. Three-dimensional imaging of macular inner structures in glaucoma by using spectral-domain optical coherence tomography. *Invest Ophthalmol Vis Sci* 2011;52(3):1412–1421.
16. Raza AS, Cho J, de Moraes CG, et al. Retinal ganglion cell layer thickness and local visual field sensitivity in glaucoma. *Arch Ophthalmol* 2011;129(12):1529–1536.
17. Quigley HA, Dunkelberger GR, Green WR. Retinal ganglion cell atrophy correlated with automated perimetry in human eyes with glaucoma. *Am J Ophthalmol* 1989;107(5):453–464.
18. Sakamoto A, Hangai M, Nukada M, et al. Three-dimensional imaging of the macular retinal nerve fiber layer in glaucoma with spectral-domain optical coherence tomography. *Invest Ophthalmol Vis Sci* 2010;51(10):5062–5070.
19. Mwanza JC, Oakley JD, Budenz DL, Chang RT, Knight OJ, Feuer WJ. Macular ganglion cell-inner plexiform layer: automated detection and thickness reproducibility with spectral domain-optical coherence tomography in glaucoma. *Invest Ophthalmol Vis Sci* 2011;52(11):8323–8329.
20. Takayama K, Hangai M, Durbin M, et al. A novel method to detect local ganglion cell loss in early glaucoma using spectral-domain optical coherence tomography. *Invest Ophthalmol Vis Sci* 2012;53(11):6904–6913.
21. Leung CK, Lam S, Weinreb RN, et al. Retinal nerve fiber layer imaging with spectral-domain optical coherence tomography: analysis of the retinal nerve fiber layer map for glaucoma detection. *Ophthalmology* 2010;117(9):1684–1691.
22. Jeoung JW, Park KH. Comparison of Cirrus OCT and Stratus OCT on the ability to detect localized retinal nerve fiber layer defects in preperimetric glaucoma. *Invest Ophthalmol Vis Sci* 2010;51(2):938–945.
23. Ooto S, Hangai M, Sakamoto A, et al. Three-dimensional profile of macular retinal thickness in normal Japanese eyes. *Invest Ophthalmol Vis Sci* 2010;51(1):465–473.
24. Hirasawa H, Tomidokoro A, Araie M, et al. Peripapillary retinal nerve fiber layer thickness determined by spectral-domain optical coherence tomography in ophthalmologically normal eyes. *Arch Ophthalmol* 2010;128(11): 1420–1426.
25. DeLong ER, DeLong DM, Clarke-Pearson DL. Comparing the areas under two or more correlated receiver operating characteristic curves: a nonparametric approach. *Biometrics* 1988;44(3):837–845.
26. Hood DC, Raza AS, de Moraes CG, et al. Initial arcuate defects within the central 10 degrees in glaucoma. *Invest Ophthalmol Vis Sci* 2011;52(2):940–946.
27. Ferreras A, Pablo LE, Garway-Heath DF, Fogagnolo P, García-Feijoo J. Mapping standard automated perimetry to the peripapillary retinal nerve fiber layer in glaucoma. *Invest Ophthalmol Vis Sci* 2008;49(7):3018–3025.
28. Kanamori A, Naka M, Nagai-Kusuhara A, Yamada Y, Nakamura M, Negi A. Regional relationship between retinal nerve fiber layer thickness and corresponding visual field sensitivity in glaucomatous eyes. *Arch Ophthalmol* 2008; 126(11):1500–1506.
29. Shoji T, Sato H, Ishida M, Takeuchi M, Chihara E. Assessment of glaucomatous changes in subjects with high myopia using spectral domain optical coherence tomography. *Invest Ophthalmol Vis Sci* 2011;52(2):1098–1102.
30. Arintawati P, Sone T, Akita T, Tanaka J, Kiuchi Y. The applicability of ganglion cell complex parameters determined from SD-OCT images to detect glaucomatous eyes. *J Glaucoma* 2012 [Epub ahead of print].

Biosketch

Yugo Kimura, MD, graduated from Hiroshima University Medical School, Hiroshima, Japan, in 2001. He completed his residency at Kyoto University Hospital. Dr Kimura is now performing clinical research at the Kyoto University Graduate School of Medicine, Kyoto, Japan. He specializes in glaucoma, and his research interests are glaucoma in highly myopic eyes and genome analysis of patients with glaucoma.